International Journal of Heat and Mass Transfer 52 (2009) 442–450

Contents lists available at ScienceDirect

International Journal of Heat and Mass Transfer

journal homepage: www.elsevier.com/locate/ijhmt

General characteristics of two-phase flow distribution in a compact heat exchanger

Mohammad Ahmad, Georges Berthoud, Pierre Mercier *

Commissariat à l'Energie Atomique, 17 rue des martyrs, 38054 Grenoble, France

ARTICLE INFO

Article history:
Received 24 April 2007
Received in revised form 25 March 2008
Available online 26 July 2008

Keywords:
Two-phase flow
Maldistribution
Compact heat exchangers

ABSTRACT

An experimental loop representing a compact plate heat exchanger was built up to study the two-phase distribution in the different header channels. The test section consists of a cylindrical horizontal header and eight rectangular channels in which the liquid and vapour flow rates are evaluated and the flow inside the header can be visualized. Several geometrical and functional parameters to study the two-phase distribution were tested using "HFE 7100" at a temperature close to 57 °C and a pressure close to 100 kPa. A flow pattern map in the header was built up using the different entry parameters on which a quantitative understanding of the two-phase distribution could be deduced.

1. Introduction

Two-phase maldistribution reduces the thermal and hydraulic performance of compact heat exchangers with parallel flow circuits and may cause the apparition of dry-out zones in evaporators and high liquid loading zones in condensers. The maldistribution in parallel circuits is significantly related to the two-phase flow patterns in the header, as well as to several other factors as the non-uniform thermal loading of different sections of the heat exchanger, fouling, corrosion, etc.

Different authors have investigated the two-phase flow distribution in compact heat exchangers. Watanabe et al. [1] studied experimentally the distribution of R11 in an evaporator of four tubes manifold and they examined the load heat effect on flow distribution. Rong et al. [2] carried out an adiabatic experiment to study the distribution of air–water flow in a horizontal manifold of vertical channels with downward or upward orientation of a compact heat exchanger used for automotive air-conditioning. Moura [3] carried out both experimental study and numerical modeling on the two-phase flow distribution between two passes of a heat exchanger. Webb and Chung [4] examined the effect of the manifold geometry and the orientation of inlet and outlet channels on the distribution. Bernoux [5] investigated experimentally the effect of inlet mass flow rate and mass quality on the two-phase distribution of a compact plate heat exchanger. Fei [6] made some experiments detecting the importance of the expansion valve position on establishing the flow configuration before plate evaporators. Vist and Pettersen [7] used circular header as horizontal inlet manifolds (inner diameter: 8 and 16 mm) with 10 parallel vertical tubes. They investigated the two-phase flow distribution of R134a in round tube manifolds with 10 parallel tubes with operating conditions (mass flux: 199–331 kg/m^2 s, quality: 0.11–0.50). The results showed that vapour phase flow was mainly distributed into the tubes near the inlet, and the liquid was preferentially distributed to the last tubes of the heat exchanger. Lee and Lee [8] examined the distribution of two-phase annular flow at header channels junctions of a compact plate heat exchanger. They focused on the effect of the intrusion depth of the channels to improve the liquid phase distribution. Jiao and Baek [9] proposed an original concept of an evaporator design adding a complementary fluid cavity in the distributor. The experimental studies showed that the maldistribution is highly affected by the distributor configuration. Rao Bobbili et al. [10] developed a mathematical model to investigate the effect of maldistribution on the thermal performance as well as the exit vapour quality of a plate heat exchanger. All the above research mentioned described the uneven distribution of the two phases in the different heat exchanger channel without eliminating its causes.

In the present study, different structural and functional parameters that can influence the distribution are investigated to get a general understanding of the two-phase distribution in a compact plate heat exchanger. A general investigation of the different two-phase flow structures in the header explains the causes of maldistribution in different test conditions and helps in designing an optimized heat exchanger.

2. Experimental apparatus

2.1. Test section

The test section consists of a horizontal header (manifold) and eight parallel downward channels (Fig. 1). The test section with eight channels can be rotated around the manifold axis so that

* Corresponding author. Tel.: +33 438783766; fax: +33 438785161.
E-mail address: pierre.mercier@cea.fr (P. Mercier).

0017-9310/$ - see front matter © 2008 Elsevier Ltd. All rights reserved.
doi:10.1016/j.ijheatmasstransfer.2008.05.030

Nomenclature

C_p	specific heat at constant pressure (J/kg K)
G	mass velocity (kg/m^2 s)
h	enthalpy (J/kg)
$\dot{M}$	mass flux (kg/h)
P	pressure (Pa)
T	temperature (K)
x	mass quality
Greek symbols	
ΔT	variation in temperature (K)
Subscripts	
e	inlet
i	tube number
l	liquid
s	outlet
SI	test section inlet
v	vapour
evap	pre-evaporator

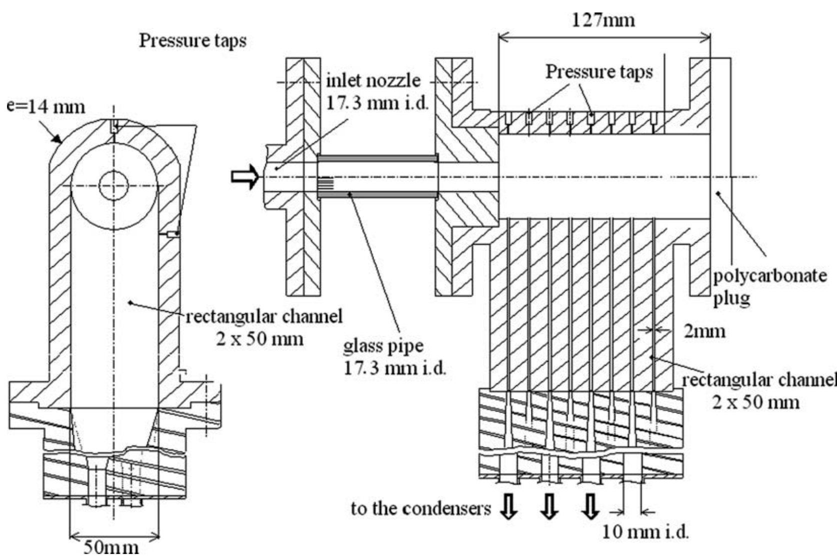

Fig. 1. Test section.

we can get horizontal flow, vertically upward or downward flow in the channels. The manifold is made of stainless steel. It is 127 mm long and its diameter is 50 mm. It is horizontally supplied by a 17.3-mm in diameter and 100-mm-long glass pipe to visualize the two-phase flow at the header inlet connected to a 1500-mm tube made of stainless steel of the same diameter. The long tube provides a steady-state flow at the header inlet. The end of the header is closed by a transparent polycarbonate plug. Each branch is 2×50 mm rectangular. The channels are regularly 10 mm spaced along the manifold.

The header diameter is reduced to 30 mm and then to 17.3 mm by introducing cylindrical devices in the main header of 30 and 17.3 mm, respectively, as inner diameters and an external diameter of 50 mm pierced at the channels level.

2.2. Flow loop and experimental procedure

The experimental loop, shown in Fig. 2 consists of four circuits: the main circuit (HFE 7100), a heating circuit of hot water (pre-evaporator), a cooling circuit of cold water with eight sub-circuits (eight condensers) and a sub-cooling circuit of cold water to assure the sub-cooling of HFE 7100 and thus to avoid the cavitation in the main circuit pump.

In the main circuit, the flow is driven by a variable speed gear pump which can facilitate the control on the flow rate. Nine heat exchangers are placed in the main loop of the experimental set-up: the pre-evaporator (upstream the test section) and the eight condensers (one downstream each channel). Four RTD (platinum temperature sensors) sensors are located at the inlet and the outlet of each heat exchanger (two on the HFE 7100 side and two on the heating–cooling water side). An absolute pressure transducer is used to measure the pressure evolution in different positions in the header and at the inlet manifold. Differential pressure transducers are used to study pressure difference in the eight channels. The HFE 7100 mass flow rate in the test section is controlled through a regulation valve upstream the pre-evaporator and is measured by a coriolis mass flow-meter. Other eight coriolis mass flow-meters are located downstream the eight condensers. The water flow rate is deduced from an electromagnetic volumetric flow-meter in the pre-evaporator circuit and a micro-oval volumetric flow-meter downstream each condenser.

The fluid "HFE 7100" is controlled to be in two-phase state at the entry of the test section with an operating saturation pressure close to the ambient pressure. The notation of the pre-evaporator or one of the eight condensers is schematized in Fig. 3. The mass quality is regulated by the pre-evaporator and is calculated at its outlet, and in a similar way in each of the eight channels, from an enthalpy balance neglecting the thermal losses as shown by the following equation:

$$x = \frac{\dot{M}_{\text{water}}\overline{C}_P\Delta T_{\text{water}} - \dot{M}_{\text{HFE}}\left[h_{\text{l}}^{\text{sat}}(T_{\text{sHFE}}) - h_{\text{l}}(T_{\text{eHFE}}, P_{\text{eHFE}})\right]}{\dot{M}\left[h_{\text{v}}^{\text{sat}}(T_{\text{sHFE}}) - h_{\text{l}}^{\text{sat}}(T_{\text{sHFE}})\right]} \tag{1}$$

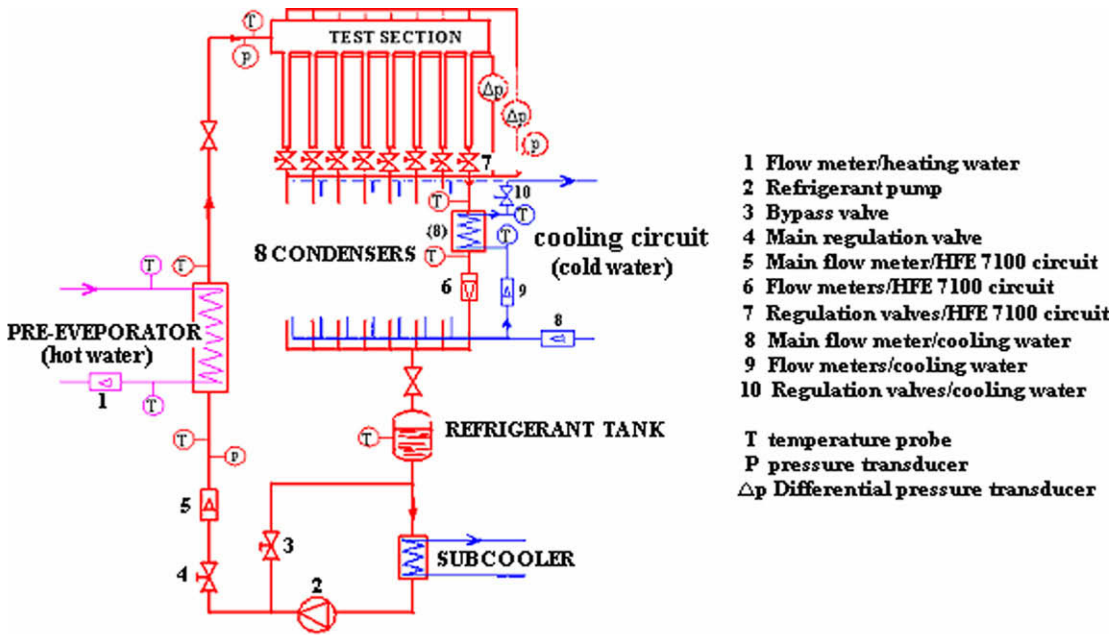

Fig. 2. Schematic diagram of the experimental apparatus.

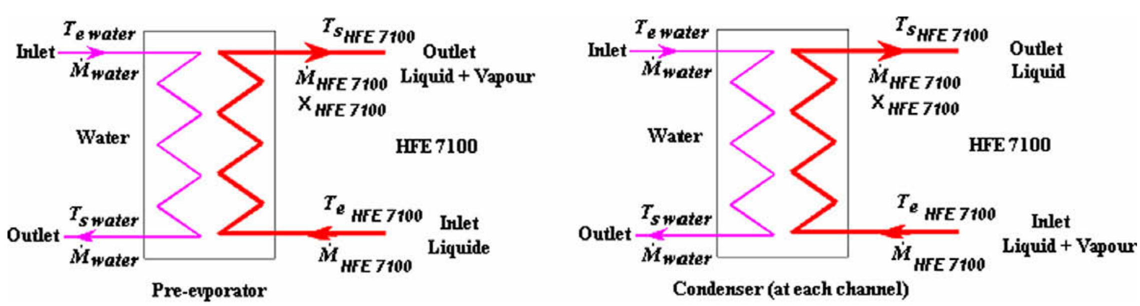

Fig. 3. Notation of the pre-evaporator and the eight condensers.

The presence of a two-phase flow state at the pre-evaporator outlet is verified by comparing the fluid enthalpy obtained from the energy balance equation and the saturation enthalpy of liquid at the outlet measured temperature. The mass quality at the test section inlet (x_{SI}) is deduced from that at the pre-evaporator outlet ($x_{s(evap)}$) considering an adiabatic flow and neglecting the change in the kinetic energy. It can be calculated as follows:

$$\dot{M}_{HFE}\left[x_{s(evap)}h_v^{sat}(T_{s(evap)}) + (1 - x_{s(evap)})h_l^{sat} \times (T_{s(evap)})\right] = \dot{M}_{HFE}\left[x_{SI}h_v^{sat}(T_{SI}) + (1 - x_{SI})h_l^{sat}(T_{SI})\right] \quad (2)$$

$$\Rightarrow x_{SI} = \frac{x_{s(evap)}h_v^{sat}(T_{s(evap)}) + (1 - x_{s(evap)})h_l^{sat}(T_{s(evap)}) - h_l^{sat}(T_{SI})}{h_v^{sat}(T_{SI}) - h_l^{sat}(T_{SI})} \quad (3)$$

2.3. Experimental conditions and uncertainty

The first tests are carried out with the reference geometry (vertically down channels and 50 mm header diameter) testing the effect of the inlet flow rate and mass quality on changing the flow configuration in the header and on the distribution. Inlet flow rates and quality ranges were 70–400 kg/m^2 s and 0.05–0.45, respectively. Different distribution channels orientations (vertically down, vertically upward or horizontal) are then investigated to trace the different possible flow structures in the header. With vertically downward distribution channels, the influence of minimizing the header diameter from 50 to 30 mm and then to 17.3 mm is examined. Expansion devices are installed at the header inlet to examine its effect on the flow structure and on distribution. All tests are performed at a temperature close to 60 °C and at a pressure close to 100 kPa except in the case where expansion devices are rigged up due to the increase in the pressure drop.

The measurement uncertainties of HFE 7100 and water flow rates are, respectively, ±0.3–0.1% and ±1%, at the pre-evaporator level and ±1–0.3% and ±1% at the condenser level in the study range. The uncertainty in measuring the water temperature was ±2.8%. The uncertainty in HFE 7100 temperature measurements is ±0.5% at the pre-evaporator level and ±1.4% at the condenser level. The uncertainty in the pressure measurements is less than ±0.6% in the present operating conditions. Quality calculated uncertainty is ±3% at the pre-evaporator level at ±3.3% at the condenser level.

3. Results

The mass quality is defined in Eq. (4) as the ratio of the vapour flow rate over the total flow rate:

$$x = \frac{\dot{M}_v}{\dot{M}} \quad (4)$$

In each channel, the mass flow rate is measured ($\dot{M}_i$) and the quality is calculated at the inlet of each condenser from the energy balance equation (Eq. (1)). In the presentation of the results of the two-phase distribution measurements, the flow ratio in channel i is presented in a normalized manner:

$$\dot{M}_i^* = \frac{\dot{M}_i}{\sum_{i=1}^{8} \dot{M}_i \Big/ 8} \quad (5)$$

In the same way, the non-dimensional liquid (resp. vapour) flow rate in channel i is the ratio of the liquid (resp. vapour) flow rate measured in channel i over the mean liquid (resp. vapour) flow rate:

$$\dot{M}_{ki}^* = \frac{\dot{M}_{ki}}{\sum_{i=1}^{8} \dot{M}_{ki} \Big/ 8} \quad (6)$$

where k = l (liquid) or v (vapour).

3.1. Effect of mass quality and flow rate on distribution

3.1.1. Flow pattern at the inlet and inside the header

Flow visualization is carried out by implementing a camera video technique. Fig. 4 shows the flow patterns observed at the inlet horizontal glass tube of the header. The experimental data are compared to Zurcher et al.'s [11] models that give the transition curves between the different flow regimes using Thome's map.

At low-mass quality (5–10%) and low-mass flux, the flow is purely stratified with no perturbations at the interface level. As mass inlet velocity increases and consequently the vapour velocity increases, the liquid–vapour interface is disturbed by waves travelling in the flow direction and a wavy flow is formed. As the mass velocity exceeds 300 kg/m^2 s and for a mass quality of 20%, a highly disturbed wavy flow is formed which is not perfectly confounded with Zurcher transition model.

For a higher mass quality (35–45%) and mass velocities (150–250 kg/m^2 s), an annular configuration appears with a thin film of liquid at the upper portion of the tube and a thick layer at the lower part (ring-annular) flow, as shown in Fig. 4. As the mass velocity increases further (250–400 kg/m^2 s), an annular flow with a uniform film thickness is formed.

Fig. 5 shows a flow map with the different observed flow patterns inside the header: stratified flow (S), stratified jet (JS), liquid jet (JF) and liquid film (FF) depending on the value of the mass flux and mass quality at the header inlet.

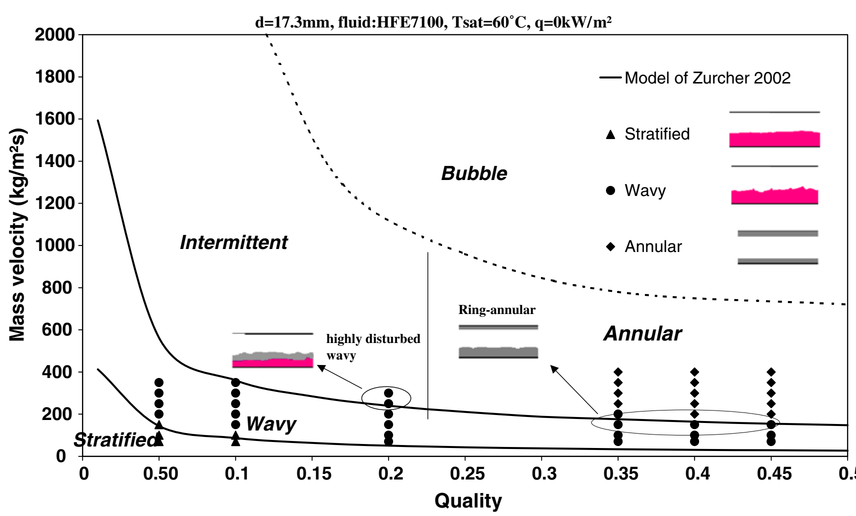

Fig. 4. Flow pattern data at the manifold inlet.

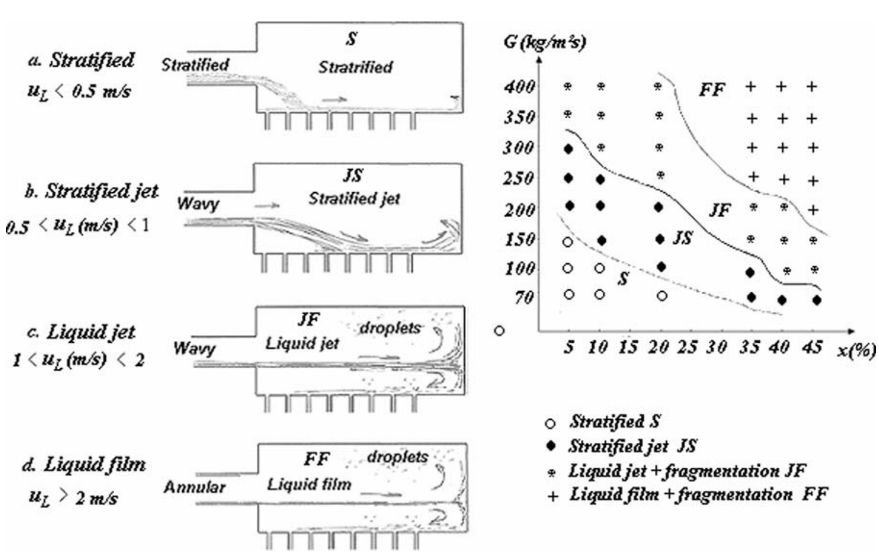

Fig. 5. Flow structure in the 50-mm diameter header.

For low-mass flux and low-mass quality, the flow is smoothly stratified at the header inlet with a weak inlet momentum (see Fig. 5a). A stratified flow will be always formed in this case inside the header and the liquid will fall into the first two channels. With the increase of mass flux, mass quality and due to the diameter enlargement at the header inlet, a liquid jet is formed. The shooting length of the jet depends on the liquid momentum. The void fraction at the inlet tube is estimated using Lockhart–Martinelli model.

At medium liquid momentum ($0.5 < u_L(\text{m/s}) < 1$), a wavy stratified flow is formed at the inlet manifold. The liquid will fall to the ground of the header, as shown in Fig. 5b with a weak jet effect, thus forming a stratified flow that will reach to the end of the header filling the channels which are on its way. In this case, no fragmentation of liquid takes place. An accumulation of liquid is observed at the header end.

At higher liquid momentum ($1 < u_L$ (m/s) < 2) when the inertia force dominates the gravity, the liquid jet traverses the entire header impacting at its end (Fig. 5c). After the impact, a part of the liquid phase is dispersed into small droplets and a part constitutes a film produced due to jet splitting with a backward velocity.

At high quality (>35%) and when the mass inlet flux exceeds certain value (>250 kg/m^2 s), an annular flow appears in the inlet tube where the vapour is surrounded by a thin film of liquid. When it enters the header, the liquid film of high velocity ($u_L > 2$ m/s) will remain intact and will continue till the end of the header where splashing takes place. However, a thin liquid film is formed in the bottom of the header end due to the accumulation of liquid in this zone.

3.1.2. Quality effect

To detect the influence of the mass quality on the two-phase distribution in the eight vertically downward channels, several experiments were carried out (Fig. 6a) with an inlet flow rate of 250 kg/m^2 s. The diameter of the inlet manifold (17.3 mm) is smaller than that of the header (50 mm). A jet is formed in the header due to this enlargement in diameter. The distribution of the liquid phase depends on the position of impact point between the liquid jet and the header. At low quality, $x = 0.05$, a liquid jet is impacting at the level of the forth channel and thus it is filled with liquid, whereas, the first and the last channels which are far from the impact point will be badly fed. At medium inlet quality, $x = 0.2$, the liquid jet trespasses all the channels and it falls on the terminal plug. In this case, the last four channels are higher fed than the first four channels. At high-inlet quality, $x = 0.45$, the liquid film traverses the header. The first two channels are better fed in this case and the liquid distribution profile is improved.

Concerning the vapour phase distribution, at low-mass quality, $x = 0.05$, no vapour passes in the forth channel which is completely fed with liquid and the last four channels are better fed with vapour. When mass quality increases to 0.2, the distribution of vapour is improved. The first set of channels are always better fed than the second set. Fig. 6a shows also that at higher mass quality, $x = 0.45$, the distribution of the vapour phase is quasi-homogeneous in the eight channels. A good influence of increasing the inlet mass quality on the two-phase distribution is observed. The best distribution corresponds to the highest inlet mass quality.

3.1.3. Mass flow rate effect on distribution

Fig. 6b shows the distribution of the vapour and liquid phases as a function of the total inlet flow rate or mass velocity. The inlet mass quality is kept constant at 20% at an inlet saturation temperature of 55 °C.

At low-mass inlet velocity, 70 kg/m^2 s, the liquid flow in the channels tends to decrease, starting with the first channel which is highly fed (more than twice the mean liquid flow rate) to the low one which is so badly fed. For the vapour distribution, the second channel is the most fed tube and the last two channels are badly fed. All the other channels are equally supplied with vapour (near to the mean vapour flow rate). At medium mass inlet velocity, 200 kg/m^{2}s, no distribution improvement was observed. The liquid tends to highly feed the last two channels. The first four channels are weakly supplied with liquid (25% of the mean liquid flow rate). A highly heterogeneous distribution of vapour is observed. At only high mass inlet velocity, 400 kg/m^2 s, the distribution of the two phases is slightly improved. The first and last channels are highly supplied with the two phases if compared with the other between-channels which are less fed. The influence of the mass inlet velocity on the distribution of the two phases is more visible only at high mass velocity.

The two-phase flow structure in the header has a significant influence on the distribution in the different channels. The more we get a homogenized multidirectional two-phase structure in the distribution box, the more uniform the two-phase distribution will be. The presence of high-momentum phases and especially that of liquid at the inlet section due to the increase of the mass flow rate and quality, favours the occurrence of impacts, fragmentation of liquid phase, and this renders the distribution more homogeneous. For low liquid momentum, the mono-directional flow tends to highly feed only a limited number of channels. This boundary configuration together with the geometrical dimensions of the distribution box is at the origin of creating the flow structures of Fig. 5 and in determining the two-phase distribution results.

3.2. Effect of header diameter

Fig. 7 shows the distribution of the liquid and vapour phases for different header diameters with an inlet quality of 20% and

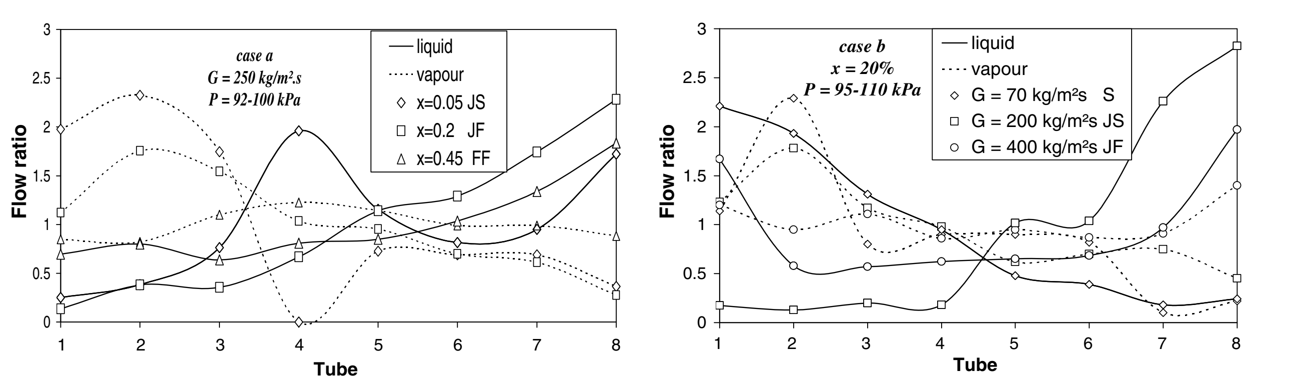

Fig. 6. Influence of the inlet quality and flow rate on the two-phase distribution. Vertically downward channel ($\phi_{header} = 50$ mm).

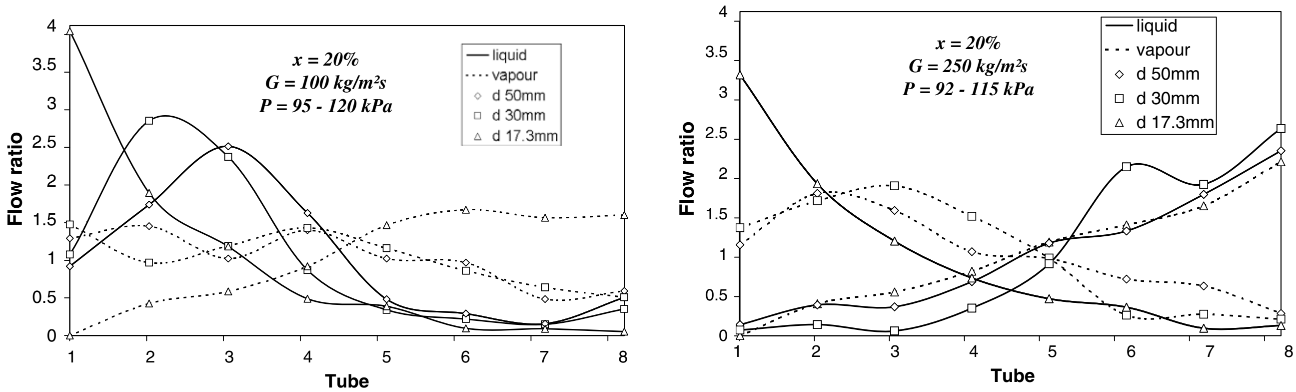

Fig. 7. Influence of header diameter on the two-phase distribution.

different mass inlet velocities (100 and 250 kg/m^2 s). At low inlet mass velocity (100 kg/m^2 s), a stratified jet is always formed if the header is greater than the inlet manifold (diameters: 30 and 50 mm). As the header diameter decreases, the jet shooting length decreases and thus the channels that are highly fed with liquid are close to the inlet section.

In the case of a 30-mm header diameter, the liquid tends to highly feed channel 2 and 3. The last four channels are badly fed (less than 40% of the mean liquid flow rate). In the case of the small header diameter (17.3 mm), the flow remains stratified inside the header (Fig. 8b and d) and the liquid is mainly taken by the first two channels. The distribution of the vapour phase in the case of 30 and 50 mm header diameter is more homogeneous than in the case of 17.3 mm header diameter where the vapour tends to badly feed the first channels.

At high inlet mass velocity (250 kg/m^2 s), a liquid jet is formed inside the 30 and 50 mm headers and a stratified flow continues constituting a thin liquid film inside the 17.3-mm header. As described in Section 3.1 for the case of a 50-mm header, the last four channels are more fed with liquid than the first four channels. When the header diameter decreases to 30 mm, the liquid is accumulated at the header end damping the arriving liquid jet (Fig. 8c). The liquid is mainly taken by the last three channels. For the smallest diameter header (17.3 mm), liquid phase as in the case of low inlet flow rate tends to high feed the first two channels.

For the vapour phase, the vapour flow fractions in the 50-mm diameter header channels are close to the mean vapour flow rate than in the other two headers.

The liquid and vapour distributions in the different flow rate cases seem to deteriorate as the header diameter decreases. The decrease in the header volume has completely changed the flow structure in the distributor. With the header diameter of 30 mm and even with a high inlet liquid momentum, the accumulation of liquid at the header end minimizes the backflow velocity of liquid after the impact and decreases the liquid dispersion and the multidirectional flow that was observed inside the 50-mm header. With the header diameter of 17.3 mm, the flow structure inside the header is similar to that at the inlet tube. The two separated phases regime seems to be dominant in small diameter headers.

3.3. Effect of channels orientation

In this section, only the channels direction of the 50-mm horizontal header was changed. The tests have been carried out with an inlet mass velocity of 200 kg/m^2 s and different inlet qualities.

3.3.1. Effect on the flow pattern inside the header

Fig. 9 shows the different flow structures observed inside the header. In the case of a horizontal channels (Fig. 9a) and at low quality (5%), the header will be half filled with liquid and no jet effect appears in this regime. As the quality increases (10% and 20%), the quantity of liquid accumulated in the bottom of header decreases and thus a liquid jet is formed. At high quality (35%), a disturbed liquid jet is formed traversing the eight channels and fragmenting after its impact on the header cap. When the quality increases more (45%), an annular flow appears in the inlet manifold and a similar liquid film inside the header like that observed in the case (Fig. 5d) of the vertically downward channel was obtained.

In the case of vertically upward channels and at low inlet qualities (5%, 10% and 20%), the header is almost filled with liquid. The vapour occupies the upper zone of the header with the appearance of a bubbly regime between the two purely single phase regimes. At higher inlet quality (35% and 45%), a liquid jet and a liquid film configurations, respectively, appear in the header.

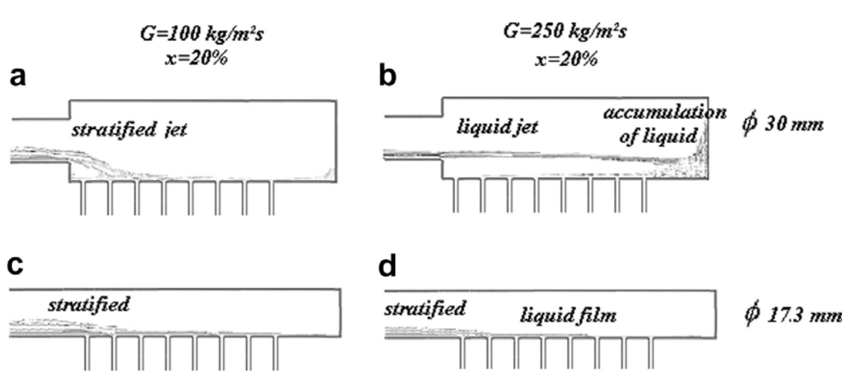

Fig. 8. Flow structure in the header of smaller diameters.

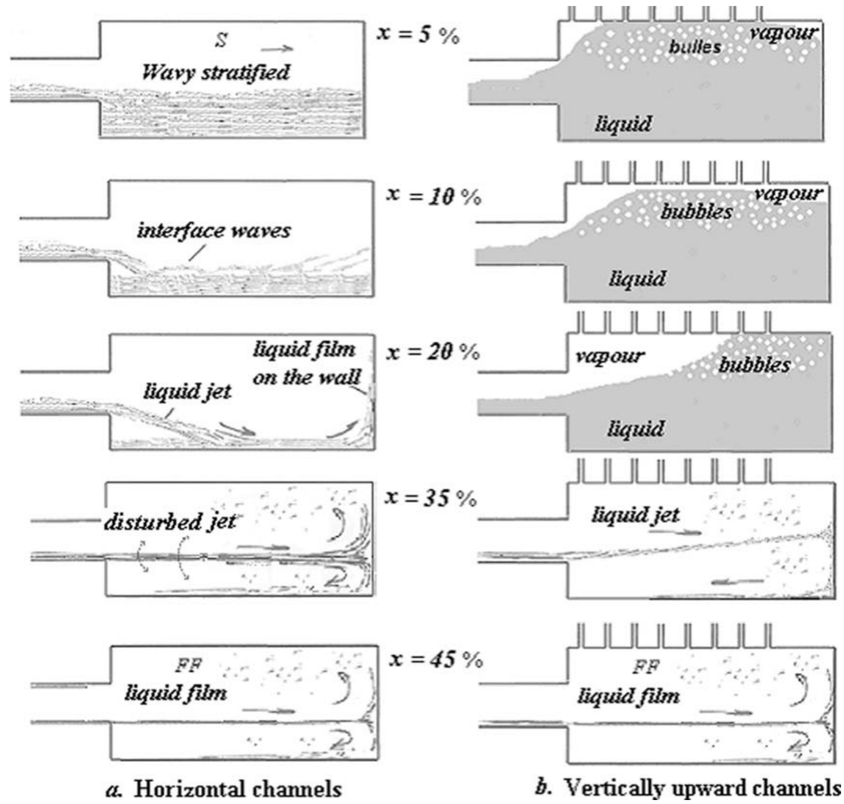

Fig. 9. Different flow structures in the manifold for different channels' orientation ($G = 200\ kg/m^2\ s$). (a) Horizontal channels and (b) vertically upward channels.

3.3.2. Effect on distribution results

Fig. 10 shows the flow distribution profiles for the three channels orientations with an inlet mass velocity of 200 kg/m^2 s and two inlet qualities (10% and 35%).

At low inlet quality (10%), the liquid phase highly supplies channels 1, 2 and 8 in the vertically upward channels header. In the vertically downward case, liquid phase moderately feeds channels 4, 5, 6 and 7 while it badly feeds the first two channels. In the horizontal channels header, the channels 4, 5, 6 and 8 are weakly fed (around 50% of the mean liquid flow rate) whereas channels 1 and 7 are fed with more than 170% of the mean average flow rate. Concerning the vapour phase distribution, the vapour is mainly aspirated by the first two channels in the vertically upward case and by the first four channels in the vertically downward case. In the horizontal case, the vapour channels supply decreases from 220% of the mean vapour flow rate for the first channel to 20% in the last one.

At high inlet quality (35%) when the channels are vertically upward, the liquid phase supplies highly the first two channels and badly the middle channels (4 and 5). In the vertically downward channels header, the liquid channels supply increases from 60% of the mean liquid flow rate in the first channel to 220% in the last one. The liquid in the horizontal case tends to feed the first two channels more than the rest. The vapour seems clearly to be more homogenously distributed in the horizontal case than the two other channels orientations cases.

The channels orientations seem to have a significant effect on the two phase distribution. At low inlet quality (10%), the liquid phase is slightly better distributed in the vertically downward case. At high inlet quality (35%), the liquid distribution is more homogenous in the horizontal case. The distribution of the two phases in the vertically upward case which is the most currently used in automobile air-conditioning heat exchangers is the less preferable. The vapour distribution is

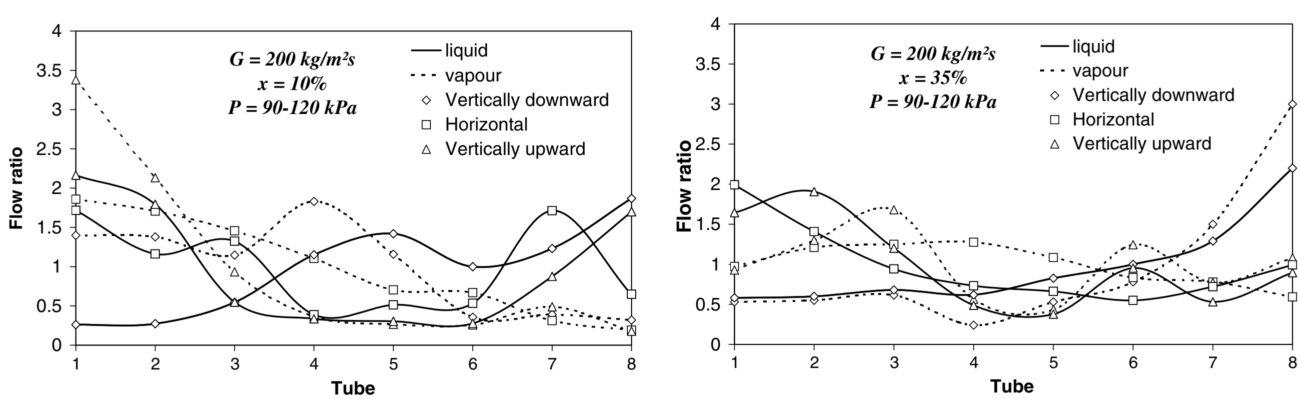

Fig. 10. Flow distribution for different channels orientation.

more homogenous in the horizontal case with high inlet quality.

3.4. Effect of the presence of expansion devices at the header inlet

The distribution of the two phases in the header channels is strongly related to the flow pattern at its inlet section. One of the main causes of the maldistribution is the presence of separated two-phase pattern at the header inlet. Expansion devices generate new configurations in the expansion region due to the pressure drop. Atomization of liquid phase takes place during the expansion and a thus homogeneous flow of vapour and small liquid droplets can be obtained. Fig. 11 shows the two expansion devices fixed at the header inlet. An atomization orifice and a splashing grid are used.

3.4.1. Flow distribution in the presence of an expansion orifice

The atomization orifice is used as an expansion device. It is made up of a single convergent hole of external diameter of 5 mm and an internal diameter of 2 mm. Due to the pressure drop exerted by the orifice, a liquid jet (Fig. 13a) is formed in the header with a high-discharge velocity. The jet atomisation or disintegration into droplets that occurs after a certain distance from the orifice depends on the discharge conditions. A droplet flow is observed downstream the jet at the header cap. A fixed small quality (5%) and pressure value are fixed before the orifice and the flow rate is changed. The quality increase after the expansion depends on the mass flow rate and the initial pressure.

For an inlet flow rate of 100 kg/m^2 s the quality in the header rises to 33% after the expansion. When the flow rate rises to 200 kg/m^2 s and then to 300 kg/m^{2}s, the quality rises to 41% and 49%, respectively. The presence of two phases before the orifice produces an interrupting jet in the header and thus a non-stationary two-phase structure. Fig. 12 shows the distribution profiles of liquid and vapour for different flow rates when the expansion orifice was used.

At low inlet flow rate (100 kg/m^2 s), the high velocity liquid jet produces pooling at the header end and thus the last channels are highly fed with liquid. At higher flow rates: 200 and 300 kg/m^2 s, the distribution of liquid was improved. An increase in the flow rate affects the flow pattern by increasing the liquid jet velocity and its shooting length. A strong rejected stream is formed after the impact in a reverse direction and decreases the pooling at the header end. The liquid phase is thus better distributed in the middle header channels for the higher inlet flow rates. An improvement of vapour distribution is also observed with the increase in the inlet flow rate.

The addition of this type of expansion devices produces a high velocity jet inside the header. If the jet velocity is not high enough, pooling at the header end occurs. As the jet velocity increases, the backflow mass increases reaching the first channels

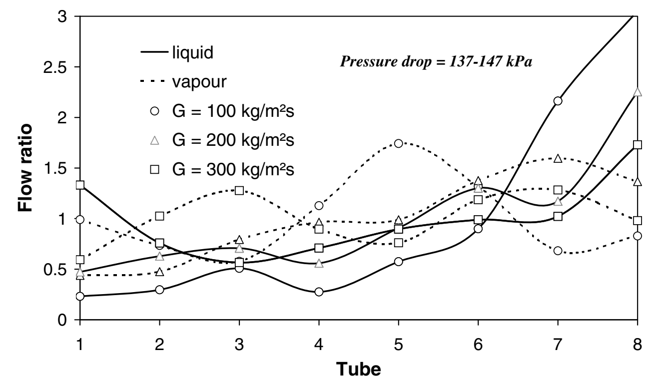

Fig. 12. Distribution profile in the presence of an expansion orifice for different inlet flow rates.

and improves the two-phase distribution. The critical needed jet velocity at the orifice exit to create a homogeneous two-phase structure inside the distribution box is function of the fluid characteristics upstream the orifice, the orifice diameter and the header geometry.

The studied case is specific by its geometrical elements but it describes the flow structure that may be created after such devices and it gives a general understanding of the relation between the obtained flow structure and the flow distribution and thus, it constitutes a starting point for adjusting different geometries.

3.4.2. Flow distribution in the presence of a splashing grid

The splashing grid is a concave plate consisting of 41 holes; the diameter of each is 0.5 mm. The concave holed surface at the header inlet provides fine droplet jets of different directions (Fig. 13b). Fig. 14 shows the distribution results obtained for different qualities and flow rates at the grid inlet. At low quality of 5% and flow rate (100 kg/m^2 s) at the grid inlet, the first and the last three channels are less supplied with liquid than the other channels.

The liquid flow ratio in each channel is bounded between 50% and 150% of the mean liquid flow rate. When the flow rate increases to 250 kg/m^2 s, the liquid distribution is slightly improved in most of the channels. Due to the pressure drop exerted by the grid, the quality inside the header increases from 5% for the two inlet flow rates (100 and 250 kg/m^2 s) to 20% and 26%, respectively. As the quality at the grid inlet increases to 20%, a remarkable improvement of liquid distribution is observed for the two tested inlet flow rates. High qualities of 43% and 47% are respectively attained inside the header in the two flow rates cases (100 and 250 kg/m^2 s).

The vapour distribution is also improved for the different inlet conditions with a maximum discrepancy of 40% of the mean liquid flow rate in each channel.

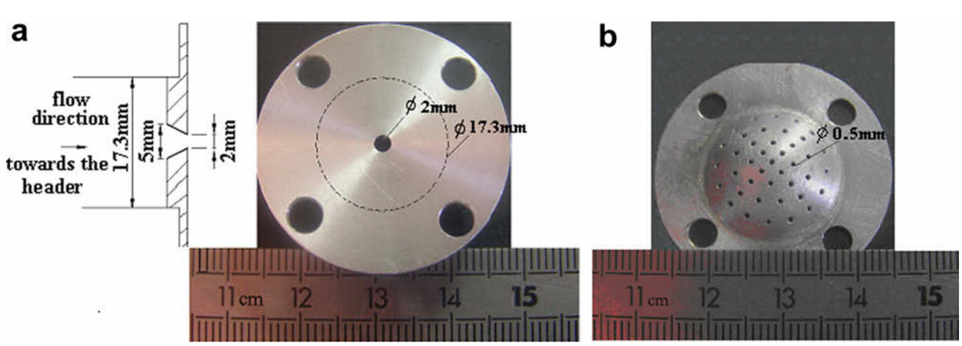

Fig. 11. Expansion devices put the header inlet. (a) Expansion orifice and (b) grille.

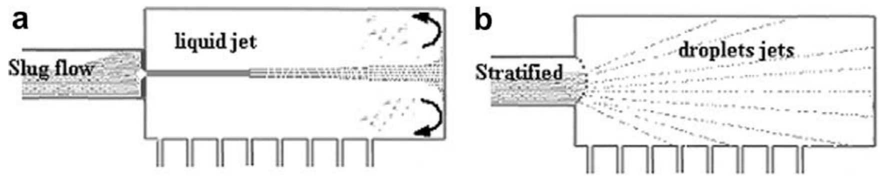

Fig. 13. Flow patterns after the two expansion devices. (a) Expansion orifice and (b) splashing grid.

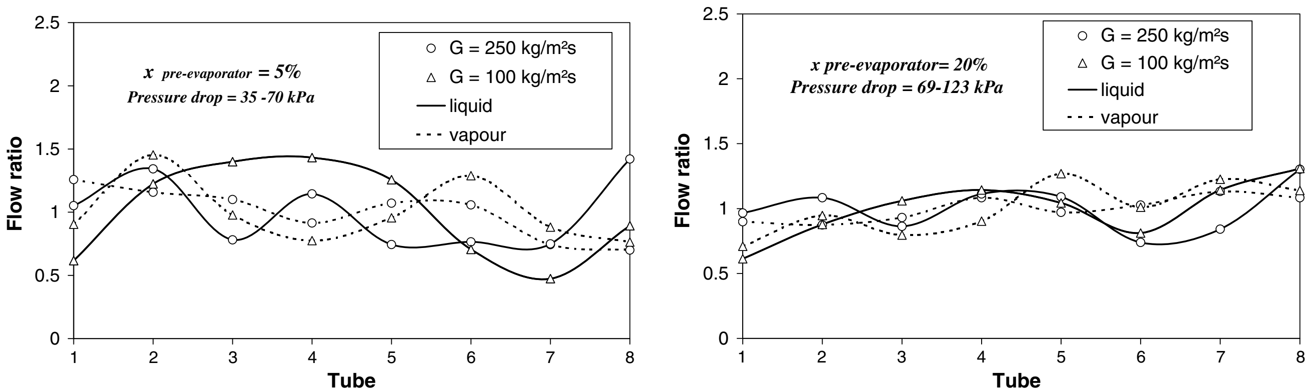

Fig. 14. Distribution profile in the presence of a splashing grid for certain inlet flow rates and qualities.

The splashing grid seems to have a remarkable influence on the two-phase distribution in the different header channels due to the liquid splattering effect and the multidirectional flow it can provide. This device can be used as a main or a secondary expansion element that follows the expansion valve.

4. Conclusions

A test section representing a manifold of a compact heat exchanger with eight channels was used in this study. The flow rate in each channel was measured and the vapour fraction was calculated by an enthalpy balance based on measurements of flow rates at the two sides of the exchanger and that of temperature and pressure.

For the case of vertically downward channels, measurement showed better a distribution for both phases as mass quality increases. The influence of the mass inlet velocity on the distribution was more visible at high mass velocity. Reducing the header diameter deteriorated the two-phase distribution.

Experiments with horizontal distribution channels showed enhanced vapour and liquid distribution even at low inlet mass quality. For the case of vertically upward channels, flow distribution was highly heterogeneous even for high inlet mass quality.

The presence of expansion devices has a great influence on the flow structure inside the header. The use of an expansion orifice produces a liquid jet configuration inside the header. High jet velocities rendered the distribution more homogeneous. The presence of a splashing grid at the inlet produces multidirectional droplets that highly improves the two-phase distribution.

The two-phase distribution in a compact heat exchanger is strictly related to the flow configuration at the header inlet and the two-phase momentum together with the header geometry. The presence of high-momentum phases and especially that of liquid favours the occurrence of impacts, fragmentation of liquid phase, the presence of a homogenized multidirectional two-phase structure and this renders the distribution more homogeneous. The present study treats certain specific geometries but the comparison between quantitative and qualitative obtained results allows the understanding of the physical phenomena of the two-phase flow inside the header and the improvement of the flow distribution by adjusting the convenient functional and geometrical parameters.

Acknowledgements

It is gratefully acknowledged that financial support for this work has been provided by CEA (Atomic Energy Commissary) and ADEME (Agency for Environment and Energy Control).

References

[1] M. Watanabe, M. Katsuta, K. Nagata, L. Sakuma, General characteristics of two-phase flow distribution in a multi-pass tube, Heat Transf. Japanese Res. 24 (1) (1995) 32–44.
[2] X. Rong, M. Kawaji, J.G. Burgers, Two-phase header flow distribution in a stacked plate heat exchanger, in: ASME Conference on Gas–Liquid Flows, FED-225, 1995, pp. 115–122.
[3] L.F. Moura, Etude de la redistribution d'un écoulement diphasique entre deux passes d'un échangeur de chaleur, Thesis CEA-GREThE, Grenoble, France, 1984.
[4] R. Webb, K. Chung, Two-phase Flow Distribution to Tubes or Parallel Flow Air-cooled Heat Exchangers, Department of Mechanical and Nuclear Engineering, University Park, Pennsylvania, USA, 2005.
[5] P. Bernoux, Etude de la distribution d'un mélange liquide–vapeur à l'entrée des échangeurs de chaleur, Thesis CEA-GREThE, Grenoble, France, 2000.
[6] P. Fei, Adiabatic Developing Two-phase Refrigerant Flow in Manifolds of Heat Exchangers, Thesis of University of Illinois at Urbana Champaign, 2003.
[7] S. Vist, J. Pettersen, Two-phase Flow Distribution in Compact Heat Exchangers Manifolds, Norwegian University of Science and Technology, N-7491, Norway, 2004.
[8] J.K. Lee, S.Y. Lee, Distribution of two-phase annular flow at header–channel junctions, Exp. Thermal Fluid Sci. 28 (2004) 217–222.
[9] A. Jiao, S. Baek, Effects of distributor configuration on flow maldistribution in plate–fin heat exchangers, Heat Transf. Eng. 26 (4) (2005) 19–25.
[10] P. Rao Bobbili, B. Sunden, S. Kumar Das, Thermal analysis of plate condensers in presence of flow maldistribution, Int. J. Heat Mass Transf. 49 (2006) 4966–4977.
[11] O. Zurcher, D. Favrat, J.R. Thome, Development of adiabatic two-phase flow pattern map for horizontal flow boiling, Int. J. Heat Mass Transf. 45 (2) (2002) 291–301.